

Universität für Bodenkultur  
University of Natural Resources and Applied Life Sciences



Institut für Lebensmitteltechnologie  
Departments für Lebensmittelwissenschaften und –technologie

## DIPLOMARBEIT

zur Erlangung des akademischen Grades Dipl.-Ing. oder DI

# Characterization of Three *Agaricus meleagris* Pyranose Dehydrogenase Isoforms

Author

Sandra Weber, Bakk. techn.

Supervisor

Haltrich Dietmar, Univ.Prof. Dipl.-Ing. Dr.techn.

Graf Michael, Dipl.-Ing. Ph.D.

Wien, September 2015



# Table of Content

Acknowledgment.....	1
Summary .....	2
Abbreviations .....	3
<b>1. Introduction.....</b>	<b>4</b>
<b>1.1 Goal of the project .....</b>	<b>4</b>
<b>1.2 Introduction to Pyranose dehydrogenase.....</b>	<b>4</b>
<b>1.3 Introduction to enzyme kinetics.....</b>	<b>6</b>
<b>1.4 Electron acceptors.....</b>	<b>7</b>
1.4.1 ABTS .....	7
1.4.2 BQ .....	8
1.4.3 $\text{Fc}^+$ .....	8
<b>2. Materials and Methods .....</b>	<b>9</b>
<b>2.1 Material .....</b>	<b>9</b>
2.1.1 Instruments.....	9
2.1.2 Chemicals.....	10
<b>2.2 Methods .....</b>	<b>10</b>
2.2.1 Enzyme purification.....	10
2.2.2 Sodium dodecyl sulfate polyacrylamide gel electrophoresis (SDS-PAGE) ....	14
2.2.3 Enzyme activity assay.....	15
2.2.4 Protein concentration .....	15
2.2.5 Characterization of PDH1, PDH2, PDH3g and PDH3y.....	16
<b>3. Results and Discussion .....</b>	<b>20</b>
<b>3.1 pH-Profiles of PDH1, PDH2, PDH3y and PDH3g.....</b>	<b>20</b>
3.1.1 Measurements with ABTS.....	20
3.1.2 Measurements with BQ.....	22
3.1.3 Measurements with $\text{Fc}^+$ .....	23
3.1.4 Comparison of the highest specific enzyme activities.....	24
3.1.5 Comparison of the specific enzyme activity at pH 7.5.....	25
<b>3.2 Measurements to determine the kinetic constants for different sugars .....</b>	<b>26</b>
<b>3.3 Determination of apparent catalytic constants .....</b>	<b>28</b>
3.3.1 PDH isoforms with electron acceptors.....	Fehler! Textmarke nicht definiert.
3.3.2 PDH isoforms with electron donors .....	31

<b>4. Conclusion .....</b>	<b>39</b>
<b>5. References .....</b>	<b>40</b>
<b>6. Curriculum vitae.....</b>	<b>42</b>

## List of Figures

Figure 1: PDH – part of 3D structure .....	4
Figure 2: Illustration of D-glucose inside the active side of PDH by [20].....	5
Figure 3: Concentration of substrate and rate relationship [7] .....	6
Figure 5: Chemical structure and reaction of ABTS [12] .....	8
Figure 6: Reaction sequence for dioxidation of D-glucose by PDH with BQ [1]....	8
Figure 7: Chemical structure of Fc [13] .....	8
Figure 8: HIC chromatogram of PDH1 - V511W.....	12
Figure 9: IMAC chromatogram of PDH1 °.....	14
Figure 10: pH dependence of the specific activity of PDH with ABTS .....	21
Figure 11: pH dependence of the specific activity of PDH with BQ .....	22
Figure 12: pH dependence of the specific activity of PDH1 with Fc <sup>+</sup> .....	23
Figure 13: PDH isoforms with ABTS as electron acceptor .....	28
Figure 14: PDH isoforms with BQ as electron acceptor .....	28
Figure 15: PDH isoforms with Fc <sup>+</sup> as electron acceptor.....	29
Figure 16: PDH isoforms with D-allose.....	31
Figure 17: PDH isoforms with D-galactose.....	31
Figure 18: PDH isoforms with D-glucose.....	32
Figure 19: PDH isoforms with Lactose .....	32
Figure 20: PDH isoforms with D-Maltose .....	33
Figure 21: PDH isoforms with Maltotriose .....	33
Figure 22: PDH isoforms with Mannose .....	34
Figure 23: PDH isoforms with Methyl- α -D-glucopyranoside .....	34
Figure 24: PDH isoforms with D-xylose .....	35

## List of Tables

Table 1: HIC buffers .....	11
Table 2: IMAC buffers .....	13
Table 3: Britton-Robinson buffer.....	16
Table 4: Dilutions of the samples .....	17
Table 5: Preparation for monitoring the activity with different sugars .....	17
Table 6: Measurement conditions to determine the kinetic constants for different sugars .....	18
Table 7: Comparison of the highest specific enzyme activities in U/mg .....	24
Table 8: Comparison of the specific enzyme activity at pH 7.5 in U/mg .....	25
Table 9: specific activity, blank corrected, undiluted; $\text{Fc}^+$ as electron acceptor; values in [U/mg] .....	26
Table 10: relative activity, blank corrected, undiluted; Glc activity of respective PDH = 100% .....	26
Table 11: Apparent kinetic constant of PDHs for selected electron acceptor .....	29
Table 12: Apparent steady state constants of PDH1 with electron donors.....	36
Table 13: Apparent steady state constants of PDH2 with electron donors.....	37
Table 14: Apparent steady state constants of PDH3y with electron donors .....	37
Table 15: Apparent steady state constants of PDH3g with electron donors.....	38

## Acknowledgment

An dieser Stelle möchte ich mich bei all jenen bedanken, die durch ihre fachliche und persönliche Unterstützung zum Gelingen dieser Diplomarbeit beigetragen haben.

Mein besonderer Dank gilt Herrn Univ.Prof. Dr. Dietmar Haltrich für das Bereitstellen dieses interessanten Themas zur Diplomarbeit und die freundliche Unterstützung die er mir entgegenbrachte.

Ebenso danke ich Herrn Dipl.-Ing. Ph.D. Michael Graf für die Betreuung und dafür, dass er mich mit all seinen Mitteln unterstützt hat, denn ohne seine Hilfe und Bemühungen wäre diese Arbeit nicht zustande gekommen.

Danken möchte ich außerdem den Mitarbeitern des Instituts für Lebensmitteltechnologie / Lebensmittelbiotechnologie für ihre Unterstützung.

Mein besonderer Dank gilt auch meiner Familie, insbesondere meinen Eltern und meinem Verlobten, die mir mein Studium ermöglicht und mich in all meinen Entscheidungen unterstützt haben.

Schließlich danke ich meinen Freunden während der Studienzeit für wunderschöne Jahre auf der BOKU.

## Summary

Pyranose dehydrogenase (PDH) is a monomeric, glycosylated flavoprotein of around 65 kDa containing covalently bound FAD. As fungal flavin dependent sugar oxidoreductase PDH probably fulfills similar biological functions in lignocellulose breakdown as fungal pyranose oxidase and cellobiose dehydrogenase, which are structurally and catalytically related [1].

In addition to *pdh1*, Roman KITTL et al. (2008) discovered two similar genes in *Agaricus meleagris* (*pdh2*, and *pdh3*), which all display a highly similar sequence. Because of their high similarity to the *pdh1* gene from *A. meleagris* and the *pdh* gene from *A. xanthoderma*, *pdh2* and *pdh3* most likely encode enzymes with PDH activities. Previous attempts to confirm this have been unsuccessful, as no active PDH2 or PDH3 protein could be obtained in sufficient amounts [2].

In the present study, we investigated the catalytic properties of PDH1, PDH2, and PDH3. Depending on the expression strategy, two differently colored pools of PDH3 were obtained, which were depicted PDH3y and PDH3g, due to their yellow or green color, respectively. These PDH isoforms were produced, purified and kinetically characterized. The obtained data were compared to each other to get insights about why *A. meleagris* produces three highly similar PDH enzymes. The results indicate predominantly a difference between the catalytic efficiencies for electron acceptors.

## Abbreviations

ABTS	2,2'-azino-bis(3-ethylbenzthiazoline-6-sulfonic acid)
1,4-BQ or BQ	1,4-benzoquinone
conc.	concentration
EF	enzyme factor
FAD	flavine adenine dinucleotide
FcPF <sub>6</sub> or Fc <sup>+</sup>	ferrocenium hexafluorophosphate
Glc	D-glucose
HIC	Hydrophobic interaction chromatography
IMAC	Immobilized metal affinity chromatography
k <sub>cat</sub>	turnover number
K <sub>m</sub>	Michaelis constant
PDH	Pyranose dehydrogenase
SDS-PAGE	sodium dodecyl sulfate polyacrylamide gel electrophoresis
V <sub>max</sub>	maximum reaction rate



# 1. Introduction

## 1.1 Goal of the project

The goal of the project was to characterize two isoforms of pyranose dehydrogenase for the first time (PDH2 and PDH3, of which the latter one was present in two distinct populations, namely PDH2y and PDH3g) in terms of their kinetic differences for different electron donors and acceptors. The obtained results were compared to each other as well as to the vast amount of data that was collected previously for PDH1 [1].

## 1.2 Introduction to Pyranose dehydrogenase

Enzymes are an interesting field of study for food science, medicine and sustainable development. Chemical reactions have an activation energy that has to be overcome in order for the reaction to occur. Many enzymes work according to the Lock and Key model and are highly specific for their substrate [3].

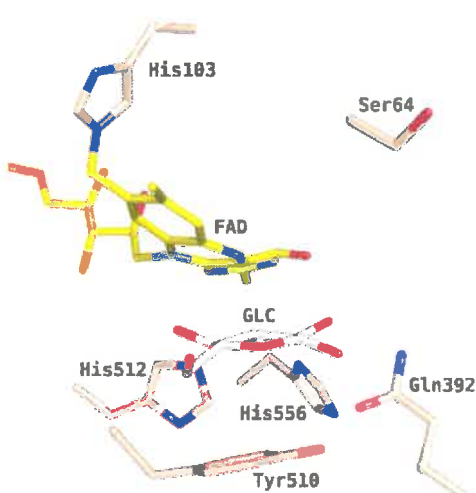


Figure 1: PDH - Part of 3D structure

PHD is a member of the structural family of GMC (glucose-methanol-choline) oxidoreductases and was only recently discovered. First, it was isolated from the edible mushroom *Agaricus bisporus*, later from the basidiomycete fungi *A. xanthoderma* as well as from *A. meleagris* and *Macrolepiota rhacodes*.

Pyranose dehydrogenase belongs to the enzyme-class of oxidoreductases. It is structurally and catalytically related to fungal pyranose oxidase and cellobiose dehydrogenase. They all probably fulfill similar biological functions in lignocellulose breakdown [1].

The monomeric, glycosylated flavoprotein PDH is composed of 577 amino acids after secretion and has a molecular mass of 65 400 Da as determined by MALDI MS [4]. The prosthetic group FAD is covalently bound *via* His-103 in the native enzyme, which is a relatively rare phenomenon because only approximately 10% of all flavoproteins are estimated to contain covalently bound flavin [5]. In 2014, Krondorfer [6] created the mutant H103Y. Although the FAD was no longer covalently linked to PHD, it still integrated itself correctly into the enzyme and PHD remained catalytically active. However, the rate if the reductive half reaction was reduced by three orders of magnitude while the oxidative half reaction was only slightly affected.

PDH uses (substituted) quinones or complexed metal ions as electron acceptor, because PDH is, unlike the closely related pyranose-2-oxidase, unable to utilize dioxygen [6].

PDH performs selective monooxidations at C-1, C-2, C-3, or dioxidations at C-1,2, C-2,3 or C-3,4 of a broad range of mono-, oligosaccharides and glycosides to the corresponding aldonolactones (C-1), or (di)dehydrosugars, depending on the structure of the sugar in pyranose form and the enzyme source [1].

Altogether, there are three PDH isoforms, namely PDH1, PDH2 and PDH3. Previously, Kittl et. al investigated the expression levels of the corresponding *pdh* genes. The identical and shared amino acids between the three isoforms are as follows: PDH1 and PDH2 (75% and 85%), PDH1 and PDH3 (76% and 85%), and PDH2 and PDH3 (84% and 92%) [2]. However, Kittl et. al were not able to produced the isoforms PDH2 and PDH3 in sufficient amounts.

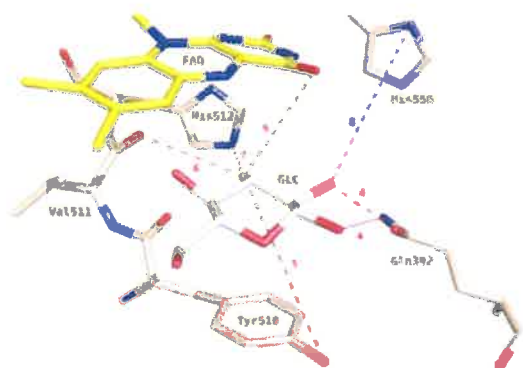


Figure 2: Illustration of D-glucose inside the active site of PDH by [20]

In this study, we produced and investigated those three PDH isoforms to get more information about their kinetic differences for different electron donors and acceptors.

### 1.3 Introduction to enzyme kinetics

The time dependent chemical reactions that are catalyzed by enzymes is called enzyme kinetic.

#### Michaelis Menten

The  $K_m$ -value is equivalent to the concentration of the substrate at  $\frac{1}{2} V_{max}$ .  $K_m$  is a very important characteristic of an enzyme and important for its biological function. The maximal reaction velocity  $V_{max}$  reveals the turnover number  $k_{cat}$ .  $k_{cat}$  shows the number of substrate molecules converted into product per active site in a certain time, if the enzyme is fully saturated with substrate [7].

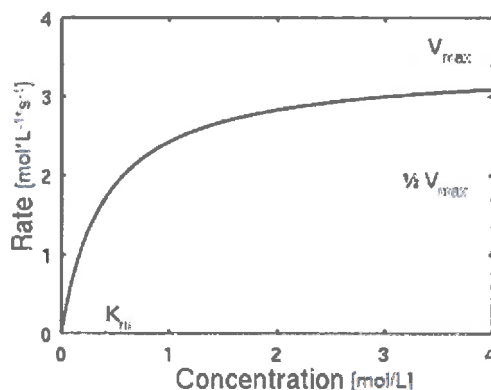


Figure 3: Concentration of substrate and rate relationship [7]

The function in figure 3 shows that the rate of the enzyme catalyzed reaction approaches a maximum ( $V_{max}$ ) when the substrate concentration is sufficiently high [8].

It can be described with the Michaelis-Menten equation:

$$v_0 = \frac{v_{max} * [S]}{K_{PT} + [S]}$$

Figure 4: Michaelis-Menton equation

S is the substrate concentration with the unit [mol·L<sup>-1</sup>].

$V_0$  and  $V_{\max}$  are the reaction rate at the beginning, and the maximum theoretical reaction rate. Their units are  $[\text{mol} \cdot \text{L}^{-1} \cdot \text{s}^{-1}]$  [7] .

$K_m$ , called the Michaelis-Menten constant, is equivalent to the concentration of the substrate at half of  $V_{\max}$ , dependent on the type of enzyme, substrate, pH and reaction temperature.

$k_{\text{cat}}$  is the turnover number. It is the maximum amount of substrate molecules converted to product per enzyme per second. Its unit is  $[\text{s}^{-1}]$  [9].

$k_{\text{cat}}/K_m$  measures how efficiently the enzyme converts the substrate into its product. Its unit is  $[\text{M}^{-1} \cdot \text{s}^{-1}]$  [9].

## 1.4 *Electron acceptors*

Only a limited group of electron acceptors work with PDH. PDH is unable to utilize  $\text{O}_2$  as an electron acceptor such as  $\text{P}_2\text{O}$ , however, it can utilize (substituted) quinones, complexed metal ions and some radical species.

### 1.4.1 ABTS

2,2'-azino-bis(3-ethylbenzothiazoline-6-sulphonic acid) or ABTS is a 1-electron acceptor substrate, which produces the blue cation radical during the reaction depicted in figure 5, by utilizing e.g. hydrogen peroxide and horse radish peroxidase (HRP). The cation radical can be read spectrophotometrically at 420 nm. Its molecular weight is 514.6 g/mol and is solvable in water [10], [11].

We used the reaction the other way round. We produced the ABTS cation radical by addition of laccase and  $\text{O}_2$ . The enzymatic activity was monitored at 420 nm spectrophotometrically by measuring the color change of the ABTS cation radical into a colorless end-product after adding PDH and D-glucose ( $\epsilon_{420 \text{ nm}} = 36 \text{ mM}^{-1} \text{cm}^{-1}$ ).

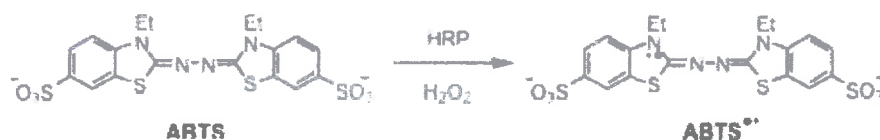


Figure 5: Chemical structure and reaction of ABTS [12]

### 1.4.2 BQ

1,4-BQ is a 2-electron acceptor. Its molecular weight is 108.09 g/mol and it can be solved in ethanol. During its reduction, catalyzed by PDH, it reacts from the yellow benzoquinone to the colorless hydroquinone (see figure 6). The absorption is measured at 290 nm ( $\epsilon_{290 \text{ nm}} = 2.24 \text{ mM}^{-1} \text{ cm}^{-1}$ ).

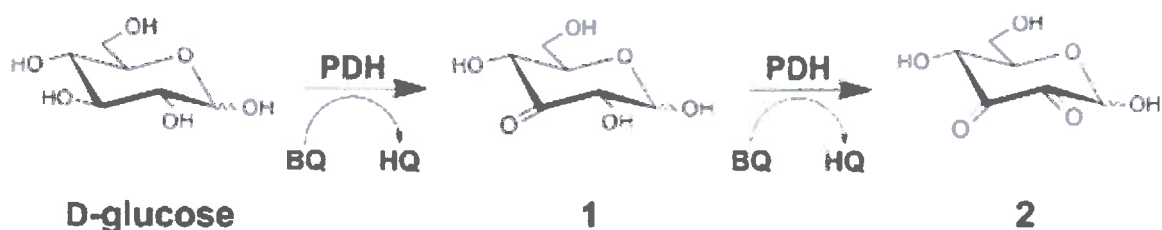


Figure 6: Reaction sequence for dioxidation of D-glucose by PDH with BQ [1]

### 1.4.3 $Fc^+$

Ferricenium hexafluorophosphate ( $FcPF_6$ ) is an electron acceptor with a dark blue appearance. It has a molecular weight of 331 g/mol and is solved in 5 mM HCl. In the used assay the electron acceptor was the ferrocenium ion ( $Fc^+$ ). PDH activity was determined spectrophotometrically following the D-glucose-dependent reduction of the ferrocenium ion ( $Fc^+$ ) to ferrocene at 300 nm ( $\epsilon_{300 \text{ nm}} = 4.3 \text{ mM}^{-1} \text{ cm}^{-1}$ ) [4].

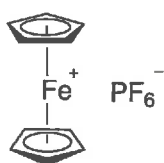


Figure 7: Chemical structure of  $Fc$  [13]

## 2. Materials and Methods

### 2.1 Material

#### 2.1.1 Instruments

Device	Manufacture	Modell
<b>Sterile work bench</b>	Thermo Scientific	Safe 2020
<b>Autoclave</b>	Kelomat	Certoklav EL 10 L/12 L
	Thermo Scientific	Varioklav
	Advantage-Lab	AL02-03 and -11
<b>Centrifuge</b>	Beckman	L-70
	Beckman-Coulter	Avanti J-26XP
	Eppendorf	5415 R
<b>Centrifuge rotor</b>	Beckman	45Ti
	Beckman-Coulter	Ja-10
	Eppendorf	1.5 mL test tubes
<b>UV-vis-spectrophotometer</b>	Perkin Elmer	Lambda 35
	Beckman-Coulter	DU800
<b>pH-meter</b>	Metrohm	744
<b>Chromatography</b>	GE Healthcare	ÄKTA prime plus
<b>Ultrafiltration tube</b>	AMICON	30 kDa cutoff
<b>Scale</b>	Sartorius Analytic	MC1 Laboratory
		LC2200S
	Sartorius Analytic	AW-224
<b>Pipettes</b>	Eppendorf / Gilson	1 µL – 1 000 µL
<b>SDS Kits</b>	BioRad Power Pac system	Power Pac HC
		Mini Protean Tetra Cell
	precast gels	4-15% Mini-Protean
		TGX Precast Gel
	Coomassie blue	G250, BioRad
<b>Vivaflow module</b>	Sartorius	VF05P2
<b>Water bath</b>	Julabo	12

<b>Refrigerator</b>		
<b>Freezer -80 °C</b>	Sanyo	MDF-J5386S
<b>Statistic software</b>	Systat	SigmaPlot™ 12.5

The presented work was done in the food biotech laboratory at the Department of Food Sciences and Technology of the University of Natural Resources and Applied Life Sciences, Vienna, Austria.

### 2.1.2 Chemicals

All chemicals used were of the highest grade available and were purchased from Merck, Sigma and Fluka.

Buffers and standards were purchased from Promega group, Bio-Rad and New England Biolabs.

## 2.2 Methods

### 2.2.1 Enzyme purification

To isolate the target protein out of a complex solution, purification in several steps was performed. The enzyme was first purified by HIC and crossflow-filtration, then by IMAC.

#### 2.2.1.1 HIC - Hydrophobic interaction chromatography

HIC separates proteins according to the differences in their hydrophobicity. The separation is based on the reversible interaction between these proteins and the hydrophobic surface of a chromatographic medium.

It is possible to expose hydrophobic parts by increasing the salt concentration since hydrophobic amino acids are mainly located in the core of the protein. The presence of certain salts in the running buffer significantly influences the interaction between hydrophobic proteins and a HIC medium.

High salt concentrations weakens the hydrate shell of the protein, thereby exposing hydrophobic amino acids and enhancing the interaction with the chromatography column. Low salt concentration weakens the interaction. With this principle, it is possible to capture the protein at high ionic strength and elute it at low ionic strength. Protein precipitation with a neutral salt, such as ammonium sulfate, is useful for purification and enrichment of a target protein from an extract without loss of activity [14], [15].

For the HIC, the sample was mixed with a saturated  $(\text{NH}_4)_2\text{SO}_4$  solution up to 40%. The HIC-column was equilibrated with buffer A (1 in Fig. 8). After the sample was loaded, the column was washed again with buffer A so that unbound proteins and other medium components were eluted from the column. This caused the  $\text{UV}_{280}$  signal to first increase and decrease afterwards when mainly the protein of interest was bound on the column. 1 mL of the flow-through was taken frequently and monitored for PDH activity and concentration (2 + 3 in Fig. 8). Afterwards, a linear elution gradient up to 100% buffer B (= elution buffer) was started within 3 column volumes (CV) and collected in 7 mL fractions (4 in Fig. 8). The fractions that contained PDH were pooled and the final volume was reduced by crossflow-filtration. In the end the column was regenerated (5 in Fig. 8). Afterwards, the sample was concentrated by crossflow-filtration and purified by IMAC.

**Table 1: HIC buffers**

<b>Buffer A – pH 6.5; 2 L</b>	
<b><math>\text{KH}_2\text{PO}_4</math></b>	<b>9.2 g</b>
<b><math>\text{K}_2\text{HPO}_4</math></b>	<b>5.6 g</b>
<b><math>(\text{NH}_4)_2\text{SO}_4</math></b>	<b>484 g</b>
<b>dissolve components in 1.9 L, set pH = 6.5 with KOH or <math>\text{H}_3\text{PO}_4</math>, fill up to 2 L</b>	
<b>Buffer B – pH 6.5; 2 L</b>	
<b><math>\text{KH}_2\text{PO}_4</math></b>	<b>9.2 g</b>
<b><math>\text{K}_2\text{HPO}_4</math></b>	<b>5.6 g</b>
<b>dissolve components in 1.9 L, set pH = 6.5 with KOH or <math>\text{H}_3\text{PO}_4</math>, fill up to 2 L</b>	



Example chromatogram:

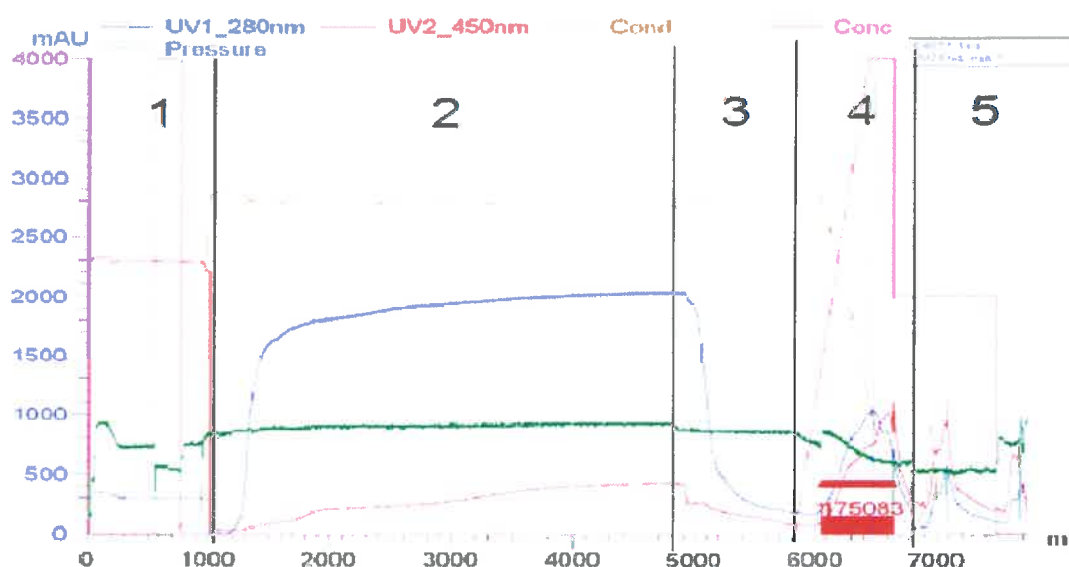


Figure 8: HIC chromatogram of PDH1 - V511W

#### 2.2.1.2 Crossflow-filtration of pooled fractions

For IMAC only small sample volumes were used. So the total volume of the pooled fractions had to be decreased. The Vivaflow module (SARTORIUS AG; Göttingen, Deutschland) with a 10 kDa cutoff was used for that. A selective enrichment in our retentate was achieved, because the size of the target protein is around 75 kDa and everything under 10 kDa passed through into the permeate. Ionic strength and pH were adapted by continuous addition of potassium phosphate buffer (50 mM, pH 7.0).

#### 2.2.1.3 IMAC - Immobilized metal affinity chromatography

By using metal chelate affinity chromatography, proteins and peptides that have an affinity for metal ions can be separated. IMAC is based on the interaction between proteins with histidine residues on their surface and divalent metal ions (e.g.,  $\text{Ni}^{2+}$ ,  $\text{Cu}^{2+}$ ,  $\text{Zn}^{2+}$ ,  $\text{Co}^{2+}$ ), immobilized via a chelating ligand. Consequently, histidine-tagged proteins have an extra high affinity in IMAC. Elution is possible with any histidine structure homologue, which has a higher affinity to the metal ion, mostly imidazole [16].

For PDH purification, a chelating Ni-Sepharose high performance medium charged with  $\text{Ni}_2^+$  was used.

Two IMAC-Columns that were connected in series were equilibrated with buffer A (1 of Fig. 9). The sample was loaded on the columns (2 of Fig. 9) and again rinsed with buffer A (3 of Fig. 9). Elution was started with a linear gradient up to 100% buffer B within 2.5 CV and the eluate was collected in 0.5 mL fractions (4 of Fig. 9).

Subsequently, a SDS-PAGE was performed with the fractions that possessed PDH-activity. Then, the fractions with the highest activity and purity of PDH were pooled and ultra filtrated in an Amicon tube (cutoff of 10 kDa) to increase the PDH concentration and reduce the volume to 0.5 mL. To change the buffer, the tube was filled three-times with phosphate buffer (50 mM, pH 7.0) and concentrated again. Protein concentration and volumetric activity of the crude extract, the flow-through, and the pooled fractions before and after ultrafiltration were measured. In the end, the column was washed (5 of Fig. 9). The concentrated PDH was sterile filtered through a 0.22  $\mu\text{m}$  membrane and 30  $\mu\text{L}$  aliquots were stored at  $-80^\circ\text{C}$ .

Table 2: IMAC buffers

<b>Buffer A – pH 7.0; 1 L</b>	
<b><math>\text{KH}_2\text{PO}_4</math></b>	13.6 g
<b>NaCl</b>	56.4 g
<b>imidazol 5mM</b>	0.34 g
<b>dissolve components in 0.9 L, set pH = 7.0 with KOH or <math>\text{H}_3\text{PO}_4</math>, fill up to 1 L</b>	
<b>Buffer B – pH 7.0; 1 L</b>	
<b><math>\text{KH}_2\text{PO}_4</math></b>	13.6 g
<b>NaCl</b>	56.4 g
<b>Imidazol</b>	34 g
<b>dissolve components in 0.9 L, set pH = 7.0 with KOH or <math>\text{H}_3\text{PO}_4</math>, fill up to 1 L</b>	

Example chromatogram:

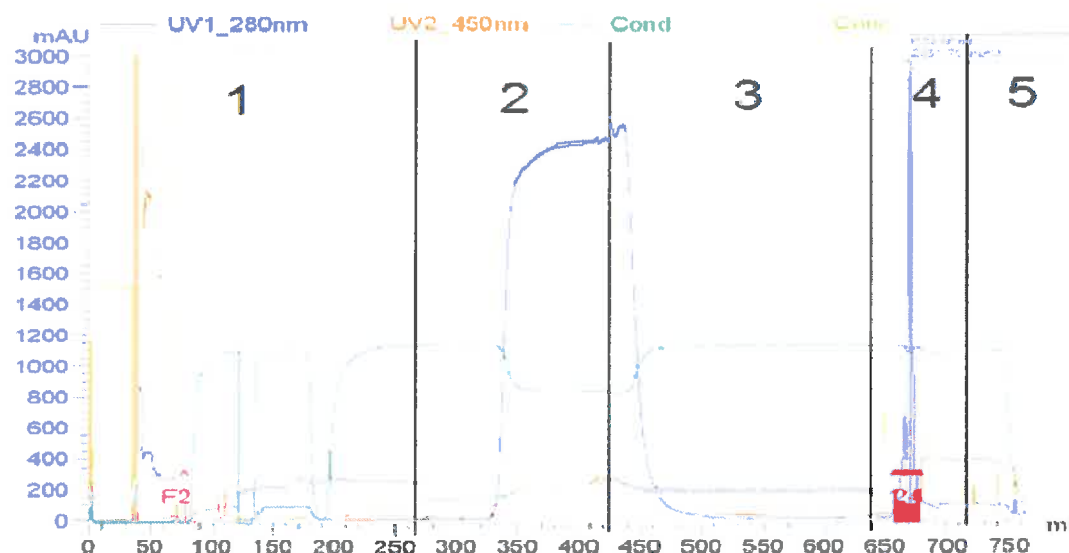


Figure 9: IMAC chromatogram of PDH1<sup>®</sup>

### 2.2.2 Sodium dodecyl sulfate polyacrylamide gel electrophoresis (SDS-PAGE)

The movement of molecules in an electric field depends on their charge and size.

SDS is an anionic detergent. By heating proteins in a buffer containing 2-mercaptoethanol and SDS, denaturation is performed without breaking peptide bonds. SDS binds strongly to all proteins and creates a constant charge to mass ratio for all denatured proteins. Mercaptoethanol reduces all disulfide bonds of cysteine residues to free sulfhydryl groups, and heating in SDS disrupts all intra- and intermolecular protein interactions. After treatment with SDS, irrespective of their native charges, all proteins acquire a high negative charge. The movement of the molecules in an electric field in a buffered polyacrylamide gel which contains SDS and thiol reducing agents is only size dependent [17].

SDS-PAGE was performed by using a BioRad Power Pac system and precast gels. 10  $\mu\text{L}$  of the protein solution with a concentration of 0.3  $\text{mg mL}^{-1}$  was mixed with 10  $\mu\text{L}$  Laemmli buffer and heated up to 95°C for five minutes. Afterwards 18  $\mu\text{L}$  of each sample was loaded in a gel pocket und was run for around 1 hour and

10 minutes at 100 V. The protein bands were visualized with Coomassie blue afterwards and background color was removed in water over night.

### 2.2.3 Enzyme activity assay

For measuring enzyme activity, enzyme assays are the method of choice. They are essential to study enzyme kinetics since they provide knowledge about the converted moles of substrate per time unit.

In the used assay, the electron acceptor was the ferrocenium ion ( $\text{Fc}^+$ ) while the electron donor was D-glucose.

PDH activity was determined spectrophotometrically following the D-glucose-dependent reduction of the ferricenium ion ( $\text{Fc}^+$ ) to ferrocene at 300 nm for three minutes at 30 °C in the standard reaction mixture (1 mL) in a cuvette. PDH continuously reduces the ferrocenium ion to ferrocene while dioxidizing D-glucose to 2,3-diketo-D-glucose [4].

For the standard reaction mixture, 770  $\mu\text{L}$  sodium phosphate buffer (65 mM, pH 7.5) and 200  $\mu\text{L}$   $\text{FcPF}_6$  (1 mM) were mixed and incubated for 10 minutes at 30°C. Afterwards the reaction was started by adding 20  $\mu\text{L}$  of the sample and 10  $\mu\text{L}$  D-glucose.

The amount of enzymes which are necessary for the reduction of 2  $\mu\text{mol}$  ferricenium ion per min under the conditions which are described above were defined as one unit of PDH activity [5].

### 2.2.4 Protein concentration

The protein concentration in solution was measured according to Bradford. We used the ready to use assay from Bio-Rad laboratories on the Backmann Coulter DU 800 Spectrophotometer at 595 nm. Bovine serum albumin was used as standard.

The used method is based on the fact that Coomassie Brilliant Blue G-250 shifts from red to blue color upon binding of the dye to protein under acidic conditions [18].

## 2.2.5 Characterization of PDH1, PDH2, PDH3g and PDH3y

### 2.2.5.1 pH-Profiles

The same conditions as for the enzyme activity assay were used, except for using Britton-Robinson buffer at various pH values instead of sodium phosphate buffer. Britton-Robinson buffer is a universal pH buffer and can be used for the pH range between 2 to 12. As electron acceptors,  $\text{Fc}^+$ , 1,4-benzoquinone (BQ) and the 2,2'-azinobis(3--ethylbenzthiazoline-6-sulfonic acid) cation radical (ABTS) were used.

Compound		for 1000 mL
Boric acid	$\text{H}_3\text{BO}_3$	2.47 g
Phosphoric acid; 85%	$\text{H}_3\text{PO}_4$	2.7 mL
Acetic acid, 99%	$\text{CH}_3\text{CO}_2\text{H}$	2.3 mL
Water		to 950 mL
Titrate to the desired pH-value with 1 M NaOH and add water to 1 L.		

Table 3: Britton-Robinson buffer

### 2.2.5.2 Probing the activity of PDH1, PDH2 and PDH3 towards different sugars

By using the same conditions as for the enzyme activity assay, measurements with different sugars were performed. In general, sugars were measured in 1 mL assays in cuvettes. Because of the high price for maltotriose, maltotetraose and allose, these sugars were measured in 50  $\mu\text{L}$  assays in uvettes. The cuvette-measurements lasted for 180 seconds, and the uvette-measurements for 300 or 600 seconds.

Table 4: Dilutions of the samples

	cuvettes	uvettes
PDH1	1:1500	1:3000
PDH2	1:4000	1:8000
PDH3y	1:1500	1:3000
PDH3g	1:1500	1:1000

Table 5: Preparation for monitoring the activity with different sugars

Preparation for	cuvettes	uvettes
Buffer	770 $\mu\text{L}$	30 $\mu\text{L}$
Fc <sup>+</sup>	200 $\mu\text{L}$	10 $\mu\text{L}$
Sample	20 $\mu\text{L}$	5 $\mu\text{L}$
Sugar	10 $\mu\text{L}$	5 $\mu\text{L}$

### 2.2.5.3 $K_m$ -values

By measuring the enzyme activity, the  $K_m$  and  $V_{\max}$  value can be determined.  $K_m$  values were determined with different electron acceptors and different sugars. BQ and ABTS were measured with 100 mM sodium acetate buffer (NaAc) and Fc<sup>+</sup> with borate buffer. The pH-values of the borate buffer were 8.5 and of NaAc 4.0.

To determine the catalytic constants  $K_m$ ,  $k_{\text{cat}}$  and enzyme efficiency  $k_{\text{cat}}/K_m$  the activity measurement results were plotted and evaluated in SigmaPlot™ (SYSTAT; Erkrath, Germany).

### 2.2.5.4 Preparation of ABTS cation radical

10.97 mg of ABTS were dissolved in 10 mL NaAc (pH 4.0) and 10 mL RO-water, to make it 1 mM. Then 20  $\mu\text{L}$  laccase were added and purged with O<sub>2</sub> for 15 minutes. Afterwards the reaction mixture was incubated in the dark over the night. On the next day it was ultra filtrated in an Amicon tube through a 10 kDa membrane. The concentration of the 1:10 diluted stock was 93.4  $\mu\text{M}$ , which was determined photometrically at 420 nm with an enzyme factor of 41.67. Measurements were performed with an ABTS radical-stock that was diluted such

that its concentration was 100  $\mu\text{M}$  in 1 mL assays in 1 mL cuvettes for three minutes at 420 nm and 30 °C. As buffer a 100 mM NaAc buffer (pH 4.0) was used and D-glucose was used as electron donor.

#### 2.2.5.5 Preparation of BQ

For a 10 mM stock, 0.054 g BQ were dissolved in 1 mL 96% EtOH in the ultrasonic bath and filled up to 50 mL with 100 mM NaAc buffer (pH 4.0). Measurements were performed after exactly 15 minutes incubation at 30 °C for 180 seconds at 290 nm in uvettes. The volume of the reaction mixture was 1 mL. 100 mM NaAc buffer at pH 4.0 and D-glucose as electron donor were used. The enzyme factor was 1339.

#### 2.2.5.6 Preparation of $\text{Fc}^+$

See 2.2.3

#### 2.2.5.7 Measurement conditions

Table 6: Measurement conditions to determine the kinetic constants for different sugars

	Measured in	Duration of measurement In sec.	Total volume of reaction mixture
<b>Allose</b>	cuvette	180	100 $\mu\text{L}$
<b>Galactose</b>	cuvette	180	1000 $\mu\text{L}$
<b>Glucose</b>	cuvette	180	1000 $\mu\text{L}$
<b>Lactose</b>	cuvette	180	1000 $\mu\text{L}$
<b>Maltose</b>	uvet	100 and 180	1000 $\mu\text{L}$
<b>Maltotriose</b>	uvet	300	100 $\mu\text{L}$
<b>Mannose</b>	cuvette	180	1000 $\mu\text{L}$
<b>Methyl-<math>\alpha</math>-D-glucose</b>	cuvette	180	1000 $\mu\text{L}$
<b>Xylose</b>	cuvette	180	1000 $\mu\text{L}$

All assays except allose and maltotriose were measured in cuvettes with sodium phosphate buffer (65 mM, pH 7.5) at 300nm at 30 °C. The EF was 139.53. The total volume of the reaction mixture with allose and maltotriose was 100  $\mu\text{L}$ , with all others sugars it was 1000  $\mu\text{L}$ . Maltose was measured over 100 seconds

## Materials and Methods

with PDH1 and over 180 seconds with PDH2, PDH3g and PDH3y. Maltotriose was measured over 300 seconds but values were taken till 100 seconds.  $\text{Fc}^+$  was used as electron acceptor in all measurements.



### 3. Results and Discussion

After the purification procedure, following protein concentrations were measured, which were used to determine  $k_{\text{cat}}$  values:

- PDH1            31.38 mg/mL
- PDH2            56.79 mg/mL
- PDH3y          115.68 mg/mL
- PDH3g          125.47 mg/mL

#### 3.1 *pH-Profiles of PDH1, PDH2, PDH3y and PDH3g*

The pH profile strongly depends on the electron acceptors. Measurements were recorded with three different electron acceptors:  $\text{Fc}^+$ , BQ and ABTS.

##### 3.1.1 Measurements with ABTS

Measurements were done in a pH range from pH 2 - 10 with the same conditions as described for the standard enzyme activity assay, except using 870  $\mu\text{L}$  Britton-Robinson buffer at the indicated pH value and 100  $\mu\text{L}$  ABTS instead of 200  $\mu\text{L}$   $\text{Fc}^+$ . The enzyme factor was 41.7, the absorption coefficient  $36 \text{ mM}^{-1} \text{ cm}^{-1}$  and the wave length 420 nm.

Dilutions of the samples:

- PDH1            1:1500
- PDH2            1:4000
- PDH3y          1:1500
- PDH3g          1:500

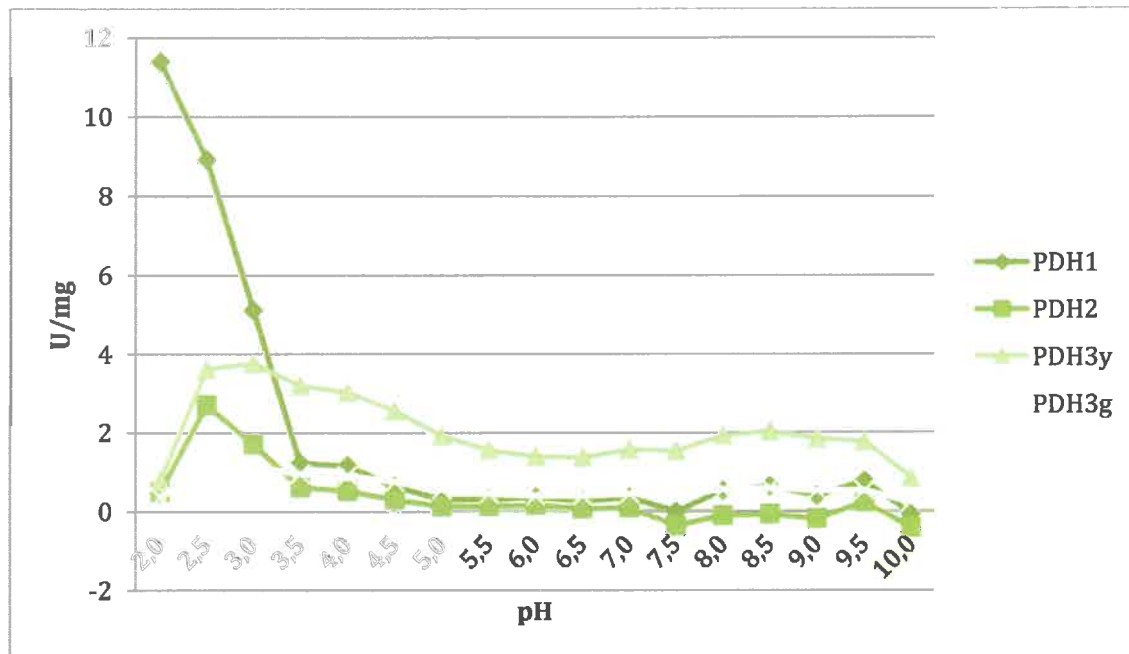


Figure 10: pH dependence of the specific activity of PDH with ABTS

PDH1 and PDH2 had their highest specific activities at very low pH values and very low to no activity from pH 3.5 towards more basic conditions.

The graphs of PDH3g and PDH3y looked similar, however, the values of PDH3y were routinely three times higher than for PDH3g. They had their highest specific activities at pH 3 and their lowest at pH 10. Between this is a local maximum in activity occurred at pH 8.5.

### 3.1.2 Measurements with BQ

Measurements were performed in a pH range from pH 2 - 10 with same conditions as described for the standard enzyme activity assay, except using Britton-Robinson buffer at the indicated pH value and BQ instead of  $\text{Fc}^+$ . The enzyme factor was 1339.3, the absorption coefficient  $2.24 \text{ mM}^{-1} \text{ cm}^{-1}$  and the wave length 290 nm.

Dilutions of the samples:

- PDH1            1:500
- PDH2            1:4000
- PDH3y          1:1500
- PDH3g          1:500

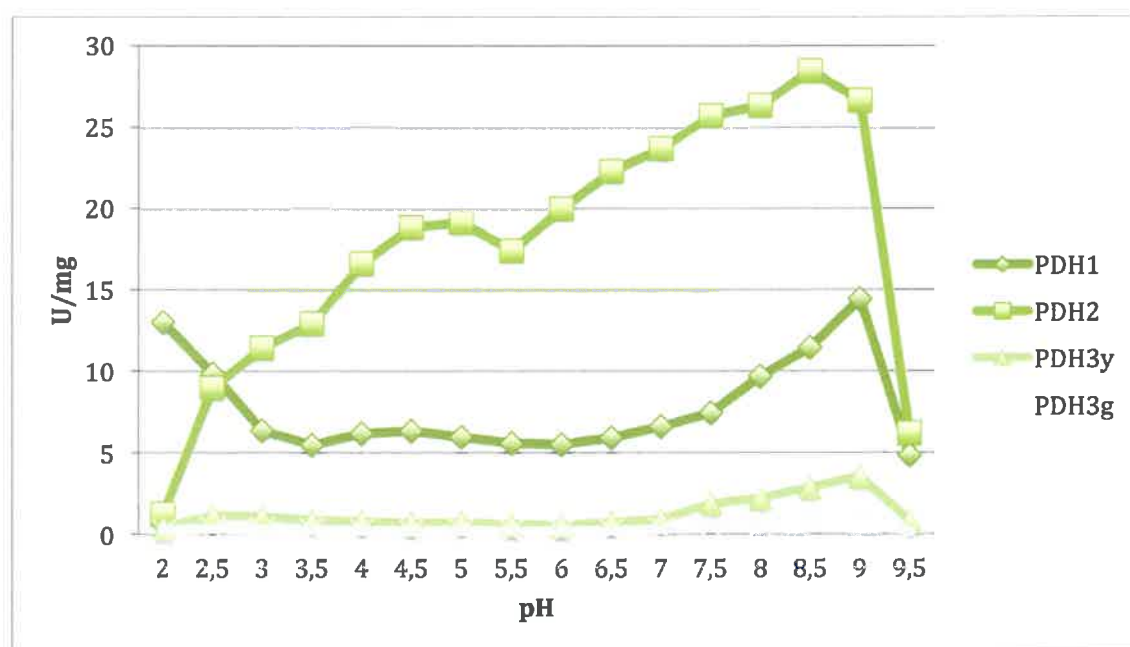


Figure 11: pH dependence of the specific activity of PDH with BQ

Using BQ as electron acceptor, PDH2 had the highest specific activity with 28.5 U/mg at pH 8.5. PDH1 had its highest activity at pH 2 and pH 9 with 13.0 and 14.4 U/mg. Between these pH values, its specific activity reached a minimum of 5.5 U/mg at pH 3.5.

The graphs of PDH3g and PDH3y again look similar. They had their highest specific activity at pH 9, where PDH3y had 3.5 U/mg and PDH3g 1.0 U/mg. Their lowest specific activity was at pH 6.

### 3.1.3 Measurements with $\text{Fc}^+$

Measurements were conducted in a pH range from pH 2 - 12 with the same conditions as described for the standard enzyme activity assay, except using Britton-Robinson buffer at the desired pH. The enzyme factor was 348.9, the absorption coefficient  $4.3 \text{ mM}^{-1} \text{ cm}^{-1}$  and the wavelength 300 nm.

Dilutions of the samples:

- PDH1            1:500
- PDH2            1:4000
- PDH3y          1:1500
- PDH3g          1:500

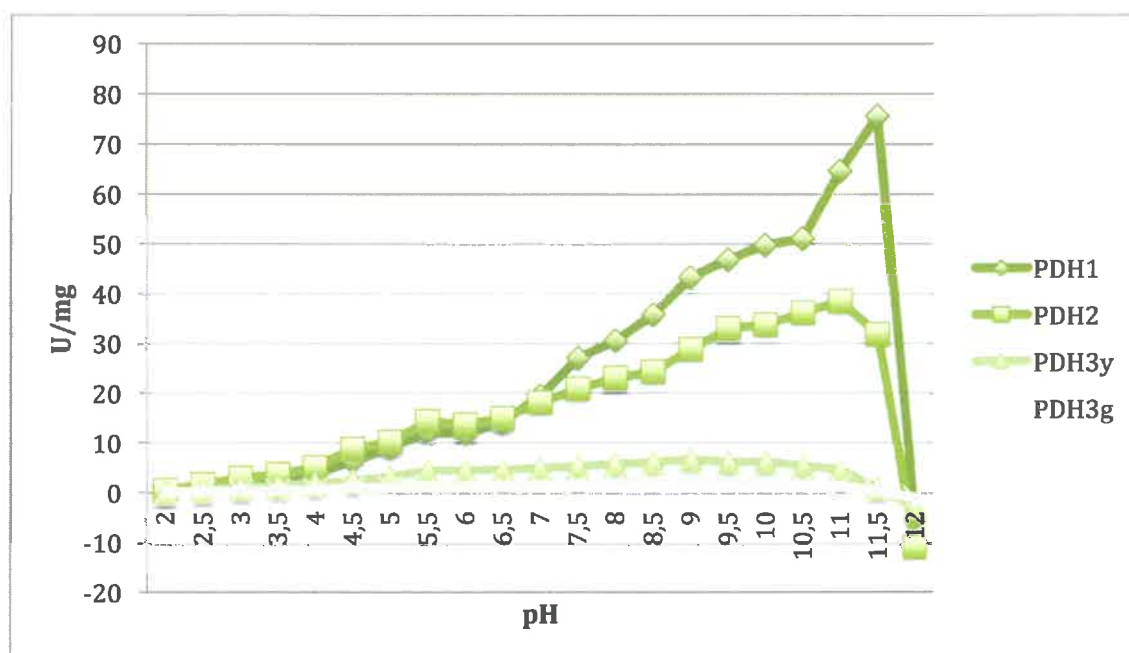


Figure 12: pH dependence of the specific activity of PDH1 with  $\text{Fc}^+$

The specific activity of PDH1 showed a significant increase until pH 11.5 and a strong decrease at pH 12. Its specific activity was the highest of all PDHs with  $\text{Fc}^+$ .

PDH2 looked similar to PDH1. Both PDH1 and isoform PDH2 exhibited maximum activity around pH 11. PDH1 showed higher relative activities than PDH2 from pH 7.0 to 11.5. At pH < 7.0 their activities were essentially the same. The pH profiles of PDH3y and PDH3g were again very similar. They had their highest specific activity at pH 9, which decreased slowly with increasing pH values until there was no measurable activity left at pH 12.

The comparison of the PDHs shows that PDH1 had the highest specific activity with  $\text{Fc}^+$  around 75 U/mg at pH 11.5. PDH2 had nearly half of its specific activity, while PDH3y only had 6 U/mg at pH 9 and PDH3g just one third of that. At pH 12 all enzymes seemed to be denatured.

### 3.1.4 Comparison of the highest specific enzyme activities

**Table 7: Comparison of the highest specific enzyme activities in U/mg**

	$\text{Fc}^+$	BQ	ABTS
<b>PDH1</b>	75.7	14.4	11.4
<b>PDH2</b>	38.6	28.3	2.7
<b>PDH3y</b>	6.7	3.5	3.7
<b>PDH3g</b>	2.1	1.0	1.1

All PDHs showed their highest specific activities with  $\text{Fc}^+$  as electron acceptor. In absolute numbers, PDH1 reached the highest enzyme activity with 75.7 U/mg.

PDH1 and PDH2 both had higher reactivities towards BQ than with ABTS, while for PDH3g and PDH3y they were higher with ABTS. In absolute numbers, PDH2 had the highest specific activity with BQ as electron acceptor, whereas they were highest for PDH1 with ABTS. The specific activities of PDH3y were always around three times higher than for PDH3g.

### 3.1.5 Comparison of the specific enzyme activity at pH 7.5

**Table 8: Comparison of the specific enzyme activity at pH 7.5 in U/mg**

	<b>Fc<sup>+</sup></b>	<b>BQ</b>	<b>ABTS</b>
<b>PDH1</b>	27.1	7.4	0*
<b>PDH2</b>	20.8	25.7	0*
<b>PDH3y</b>	5.3	1.9	1.5
<b>PDH3g</b>	1.8	0.5	0.4

\* Specific activities were set to zero if they were below zero after blank-correction

The proposed technical application of PDH is in bioelectrochemistry, e.g. for measuring blood glucose levels. Blood has a pH value between 7.35 and 7.45 [19] and therefore we compared the specific activities of the isoforms at the closest pH value, which was 7.5. All PDHs, except PDH2, work best with Fc<sup>+</sup> at that pH value. The highest enzyme activity with Fc<sup>+</sup> was 27.1 U/mg with PDH1. This is less than the half of the maximum specific activity. The specific enzyme activity of PDH2 with BQ at pH 7.5, which works best with BQ of all three isoforms, is nearly the same as at its maximum. The specific activities of PDH3y and PDH3g with Fc<sup>+</sup> are about three quarters of their respective maxima. The enzyme activity with ABTS is at a very low level for all three isoforms, however, PDH3y and PDH3g both show significant activities above the background.

### 3.2 Measurements to determine the kinetic constants for different sugars

Table 9: specific activity, blank corrected, undiluted;  $\text{Fc}^+$  as electron acceptor; values in [U/mg]

	PDH1	PDH2	PDH3y	PDH3g
<b>D-glucose</b>	21.6	21.5	3.5	1.3
<b>D-maltose</b>	14.9	2.8	0.2	0.1
<b>Maltotriose</b>	2.6	2.6	0.9	0.3
<b>Maltotetraose</b>	2.5	2.4	0.9	0.3
<b>D-mannose</b>	2.9	30.9	2.0	0.7
<b>D-allose</b>	10.0	7.5	3.5	0.7
<b>Methyl-<math>\alpha</math>-D-glucopyranoside</b>	19.8	49.5	0.5	0.2
<b>D-xylose</b>	23.0	45.7	8.1	2.6
<b>Lactose</b>	3.2	0.9	2.5	0.8
<b>L-arabinose</b>	19.9	18.9	3.7	1.2
<b>D-galactose</b>	19.1	30.2	4.2	1.5
<b>D-cellobiose</b>	15.7	10.3	2.5	0.8

Table 10: relative activity, blank corrected, undiluted; Glc activity of respective PDH = 100%

	PDH1	PDH2	PDH3y	PDH3g
<b>D-glucose</b>	100.0	100.0	100.0	100.0
<b>D-maltose</b>	68.7	13.1	5.7	4.4
<b>Maltotriose</b>	12.1	12.3	25.8	24.7
<b>Maltotetraose</b>	11.3	11.1	25.8	23.2
<b>D-mannose</b>	13.6	143.6	57.9	53.1
<b>D-allose</b>	46.3	35.0	100.2	54.8
<b>Methyl-<math>\alpha</math>-D-glucopyranoside</b>	91.7	230.2	15.6	16.3
<b>D-xylose</b>	106.5	212.5	231.4	204.5
<b>Lactose</b>	15.0	4.0	71.6	60.8
<b>L-arabinose</b>	92.0	88.1	104.6	94.6
<b>D-galactose</b>	88.5	140.2	119.2	116.4
<b>D-cellobiose</b>	72.6	47.8	72.0	63.3

In Table 10 the relative enzyme activity with glucose was set to 100% for each isoform and the activities with all other sugars are reported relative to it.

D-xylose is the only sugar for which PDH1 achieved a higher enzyme activity than for D-glucose. The enzyme activity with methyl- $\alpha$ -D-glucopyranoside, L-arabinose and D-galactose was around 10% lower than with D-glucose. The enzyme activity for the disaccharides D-maltose and D-cellobiose with PDH1 was relatively high compared to the disaccharide lactose. A reason for this could be that D-maltose and D-cellobiose consist of two D-glucose subunits, whereas lactose of one D-glucose and one D-galactose subunit. With maltotriose, maltotetraose, D-mannose and lactose PDH1 achieved only little activity.

The activity of PDH2 with methyl- $\alpha$ -D-glucopyranoside and D-xylose was more than two times increased compared to that with D-glucose. The enzyme activities with D-galactose and D-mannose were also very high compared to the activities with the other sugars, whereas there was hardly any enzyme activity with lactose. Consequently, the enzyme activity of PDH2 with disaccharides or oligosaccharides was much lower than with monosaccharide. This could be because of steric differences to the other PDHs. Maybe the substrate channel to the active site is too small for a ready accessibility of larger sugars.

As shown in Table 10, PDH3 green and yellow always had nearly the same relative activities. According to Table 10, the enzyme activity of PDH3 green was always one third of that of PDH3 yellow, with D-allose as the only exception. PDH3g and PDH3y had comparable specific activities with D-galactose, L-arabinose and D-glucose, but both enzymes worked much better, about two times faster, with D-xylose. The enzyme activity with the disaccharides lactose and D-cellobiose was relatively high, with D-maltose extremely few. An explanation for this could be the different bond-type between the two monosaccharides: lactose and D-cellobiose are connected *via* a  $\beta$ -1 $\rightarrow$ 4 glycosidic linkage, whereas D-maltose *via* a  $\alpha$ -1 $\rightarrow$ 4 glycosidic linkage. A preference for major constituents of lignocellulose such as D-glucose, D-galactose, L-arabinose and D-xylose is recognizable.



### 3.3 Determination of apparent catalytic constants

#### 3.3.1 PDH isoforms with electron acceptors

Note that the individual data points presented in this section are simply connected to each other. Therefore, the curve does represent the fit according to the Henri–Michaelis–Menten equation by nonlinear least-squares regression, which was actually used to derive the kinetic parameters.

##### 3.3.1.1 ABTS

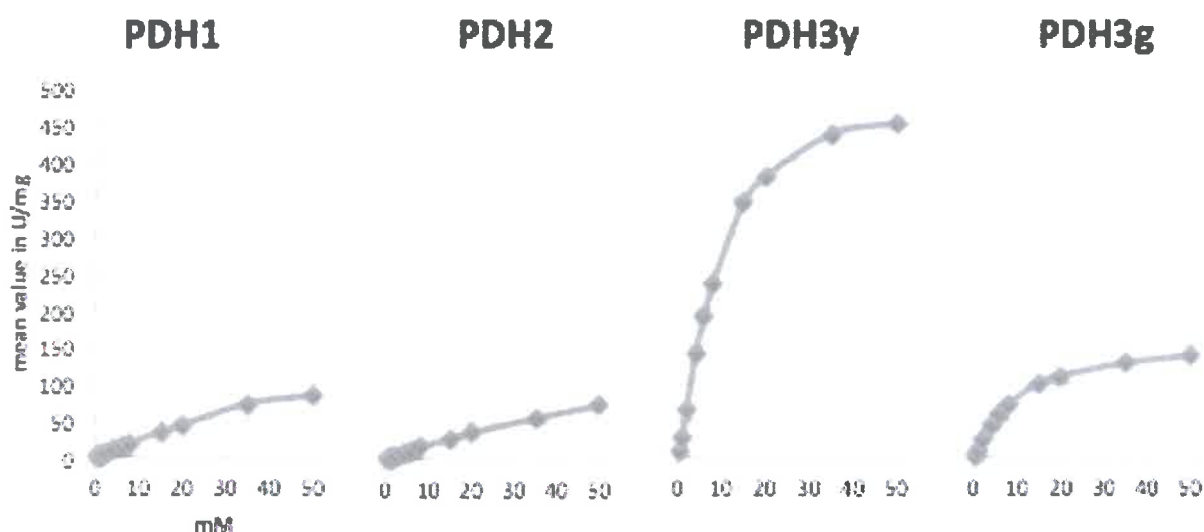


Figure 13: PDH isoforms with ABTS as electron acceptor

##### 3.3.1.2 BQ

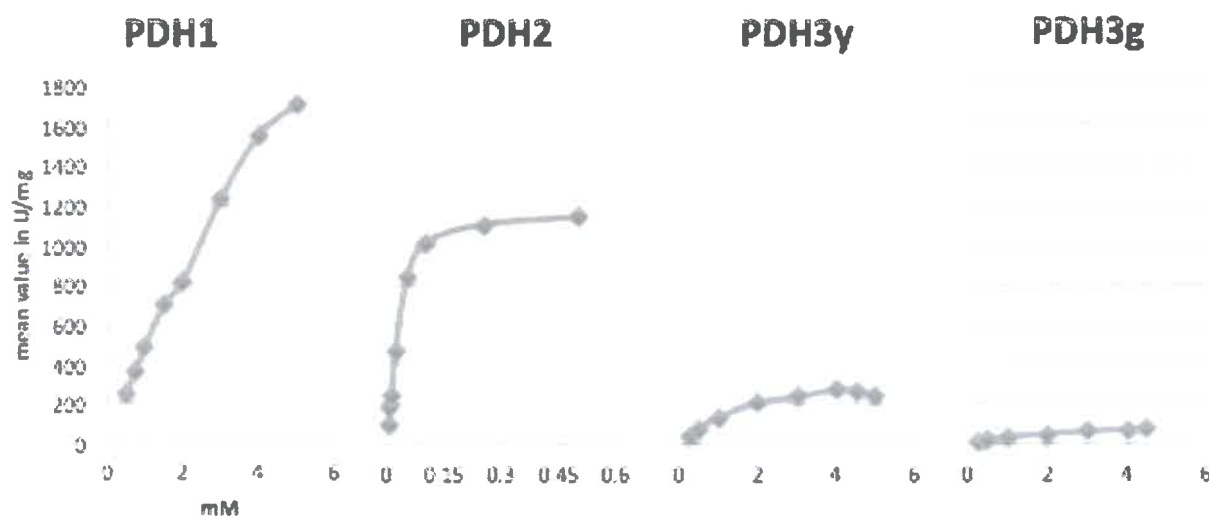


Figure 14: PDH isoforms with BQ as electron acceptor

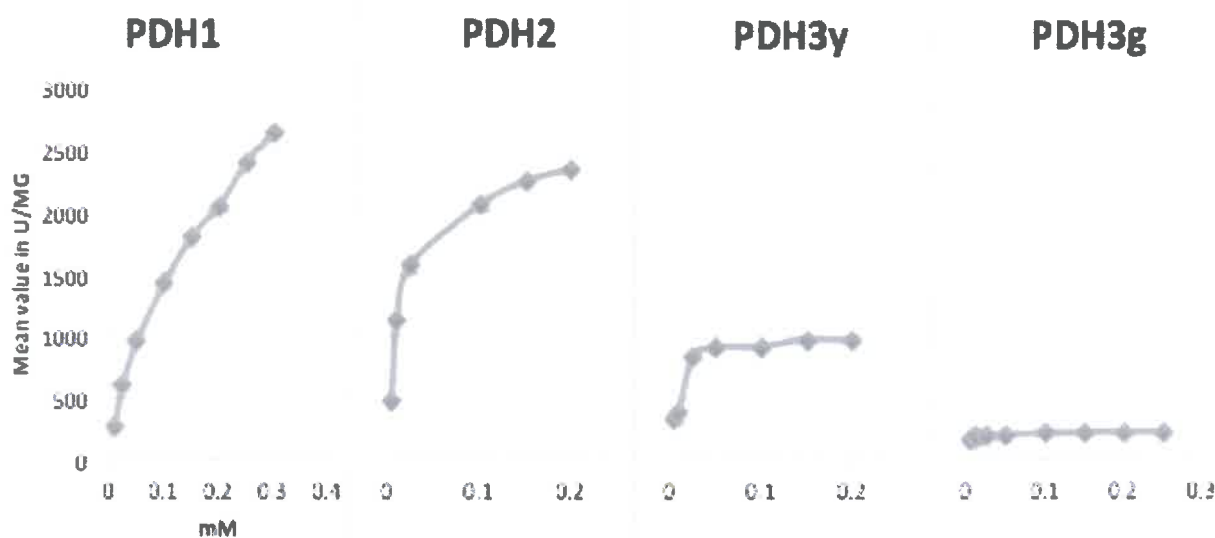
3.3.1.3  $Fc^+$ Figure 15: PDH isoforms with  $Fc^+$  as electron acceptor

Table 11: Apparent kinetic constant of PDHs for selected electron acceptor

Substrate		$V_{max}$ ( $\mu\text{mol min}^{-1} \text{mg}^{-1}$ )	$K_m$ (mM)	$k_{cat}$ ( $\text{s}^{-1}$ )	$k_{cat}/K_m$ ( $\text{mM}^{-1} \text{s}^{-1}$ )
ABTS	PDH1	$226.1 \pm 27.4$	$0.08 \pm 0.01$	7.54	92.06
	PDH2	$229.3 \pm 19.6$	$0.11 \pm 0.01$	4.26	38.94
	PDH3y	$582.8 \pm 23.5$	$0.01 \pm 0.06$	4.82	405.06
	PDH3g	$169.5 \pm 4.4$	$0.01 \pm 0.14$	1.52	134.56
BQ	PDH1	$5246.1 \pm 677.4$	$10.03 \pm 1.75$	174.95	17.45
	PDH2	$1251.7 \pm 42.1$	$0.03 \pm 0.19$	23.27	765.58
	PDH3y	$391.4 \pm 15.5$	$1.88 \pm 0.18$	3.24	1.72
	PDH3g	$111.9 \pm 3.8$	$2.20 \pm 0.17$	1.00	0.46
$Fc^+$	PDH1	$4027.5 \pm 304.2$	$0.17 \pm 0.03$	134.32	772.82
	PDH2	$2460.2 \pm 92$	$0.01 \pm 0.12$	45.75	3133.22
	PDH3y	$1055.1 \pm 54.2$	$0.01 \pm 0.13$	9.47	837.68
	PDH3g	$220.9 \pm 2.4$	$0.08 \pm 0.04$	1.98	22.13

As shown in Table 11, PDH3y had the highest affinity for the electron acceptors ABTS and  $Fc^+$ . Figure 10 indicates that the velocity of the reaction with ABTS rises extremely fast with higher substrate concentrations.

Compared to the other electron acceptors BQ and  $Fc^+$ , ABTS is less efficient

since the activity is not as high (Figures 10-12). While PDH1, PDH2 and PDHg had low activity with ABTS, PDH3y could utilize ABTS very well. This could indicate a possible steric hindrance for PDH1, PDH2 and PDH3g although this is very unlikely because of their high sequence similarity. Another explanation could be the changed microenvironment influencing the redox potential of the prosthetic FAD group, which is responsible for the electron transfer, making ABTS a suitable electron acceptor for PDH3y. Moreover, it is likely that PDH3y showed its highest activity because the measurements with ABTS took place at pH 4.0. This pH lies within the pH optimum for PDH3y and this electron acceptor (pH 2.5 to 4.0). The other isoforms had slightly shifted pH optima for ABTS: pH 2.0 for PDH1 and pH 3.0 for PDH2 or PDH3g (Figure 9).

The lowest  $K_m$  value and therefore the highest affinity for the electron acceptor BQ had PDH2. Together with its high turnover number, this resulted in a high catalytic efficiency with BQ ( $k_{cat}/K_m = 765.6 \text{ sec}^{-1}\text{mM}^{-1}$ ). While PDH3g and PDH3y had a high  $K_m$  value and did not react fast with BQ,  $V_{max}$  was not reached even with the highest possible BQ concentration for PDH1. Nevertheless, the calculated  $K_m$  value is highest for PDH1, indicating low substrate specificity. Measurements reported in chapter 3.1.2 show that PDH1 had the highest specific activity of all PDHs at pH 4.0. The pH optimum of PDH3g and PDH3y would have been at pH 9.0. Maybe that is a reason why they did not work so well. It is remarkable that the activity of PDH3g is always one third of the activity of PDH3y.

Out of all electron acceptors,  $\text{Fc}^+$  seems to be most suitable. Of all isoforms, PDH2 had highest turnover number for  $\text{Fc}^+$  ( $k_{cat} = 45.8 \text{ sec}^{-1}$ ) resulting in the best catalytic efficiency for this electron acceptor ( $k_{cat}/K_m = 3133.22 \text{ sec}^{-1} \text{mM}^{-1}$ ). PDH1 had the highest  $K_m$  value for BQ and  $\text{Fc}^+$ , whereas for PDH2 it was highest with ABTS.

Our results are in agreement with Kujawa who reported that  $\text{Fc}^+$  is one of the best electron acceptors for PDH [5]. She suspected that 1-electron substrates, like  $\text{Fc}^+$ , could be *in vivo* substrates of PDH.

3.3.2 PDH isoforms with electron donors

3.3.2.1 D-allose

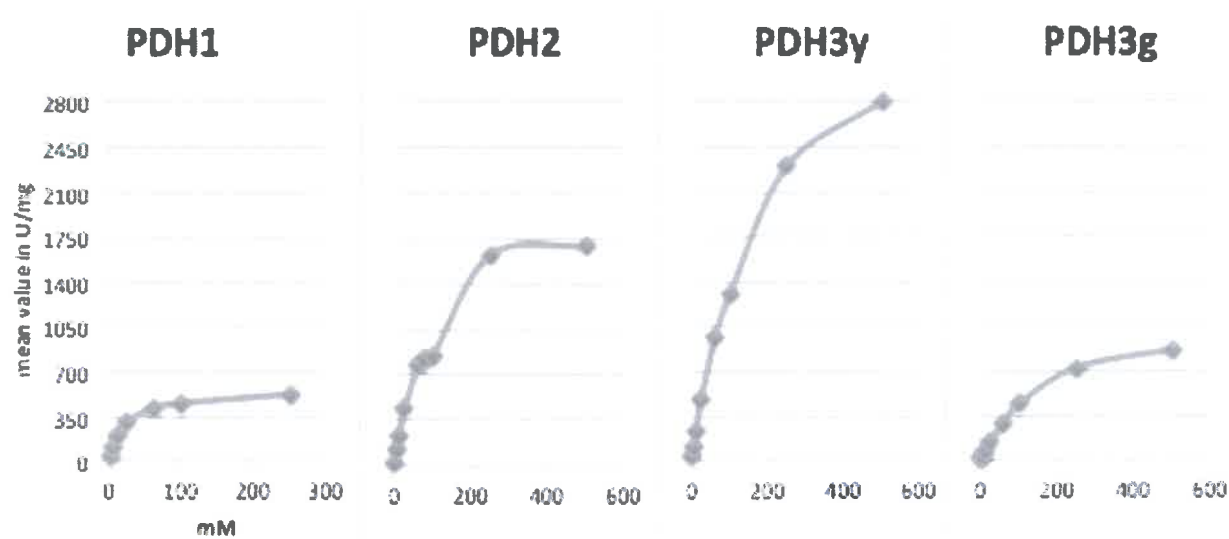


Figure 16: PDH isoforms with D-allose

3.3.2.2 D-galactose

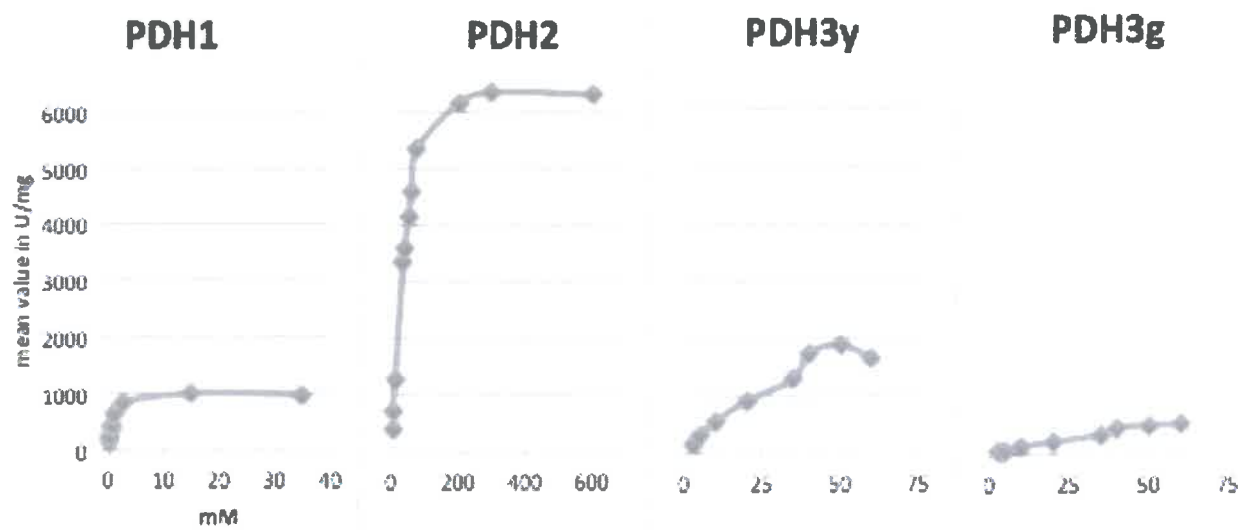


Figure 17: PDH isoforms with D-galactose

3.3.2.3 D-glucose

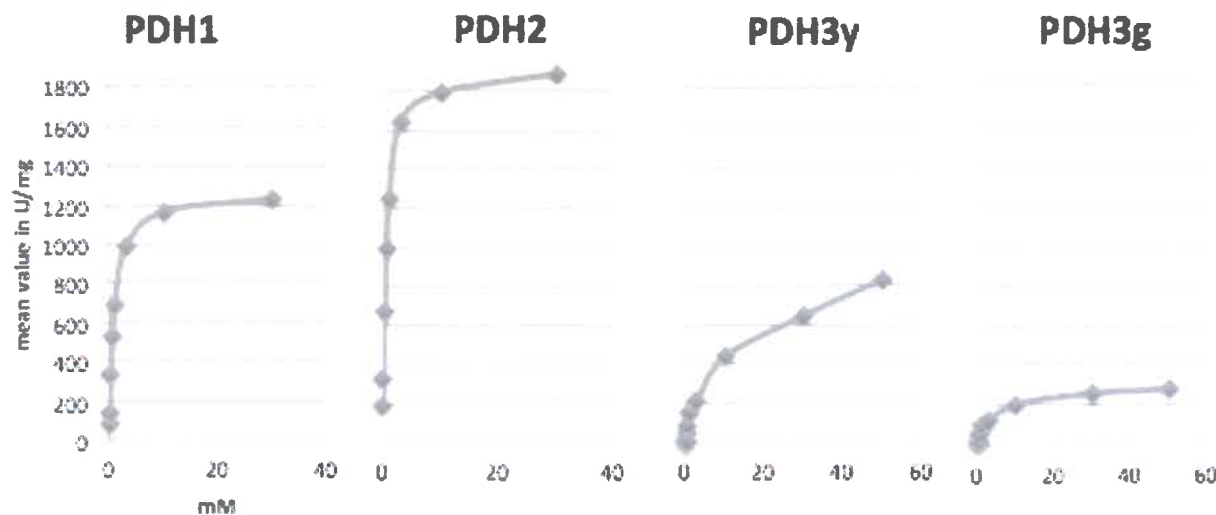


Figure 18: PDH isoforms with D-glucose

3.3.2.4 Lactose

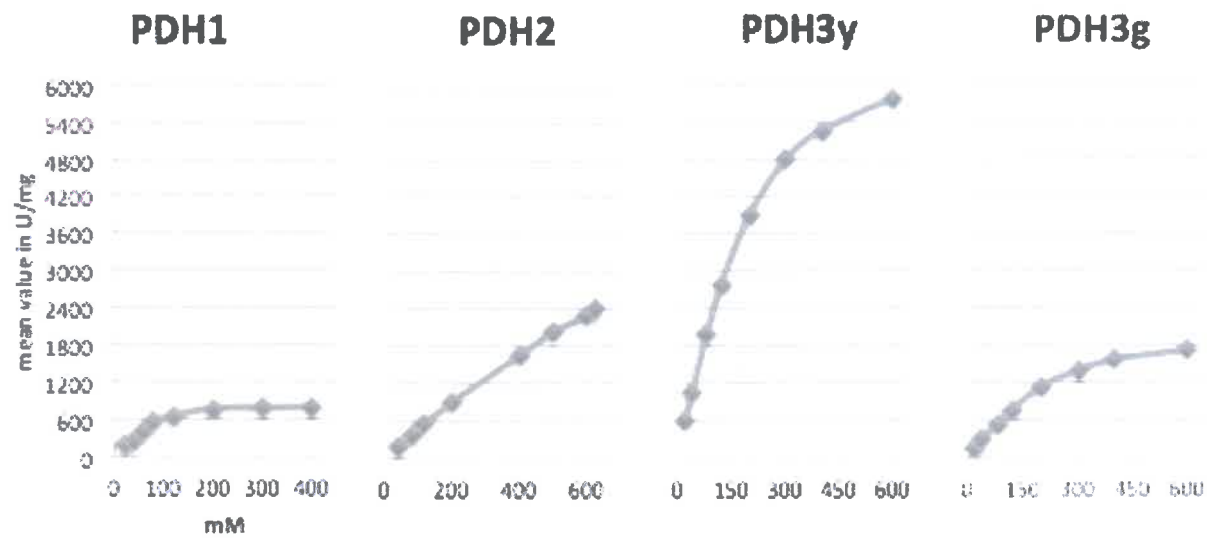


Figure 19: PDH isoforms with Lactose

3.3.2.5 D-Maltose

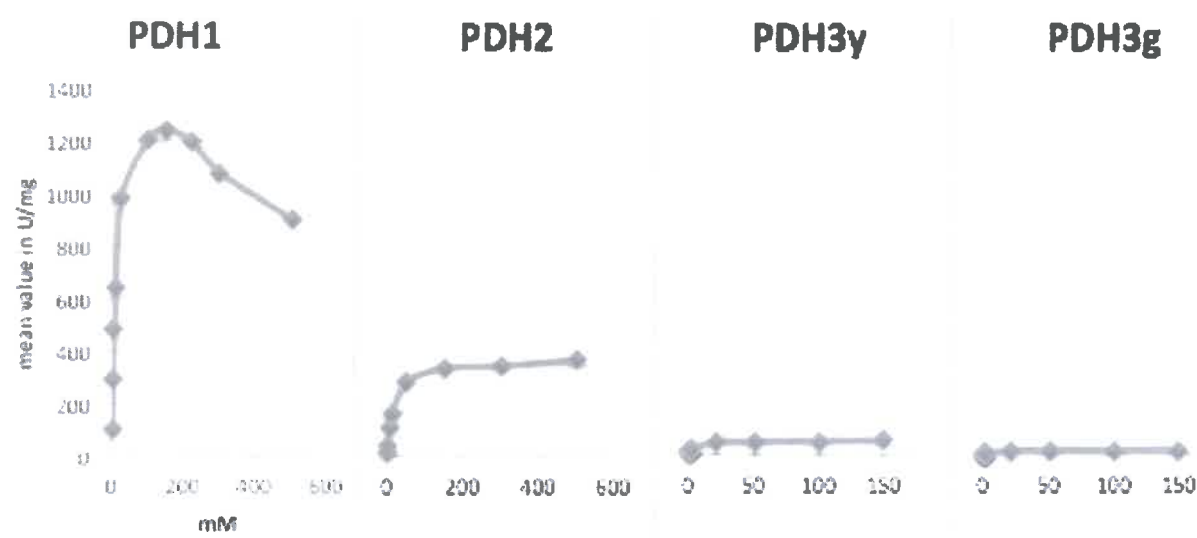


Figure 20: PDH isoforms with D-Maltose

3.3.2.6 Maltotriose

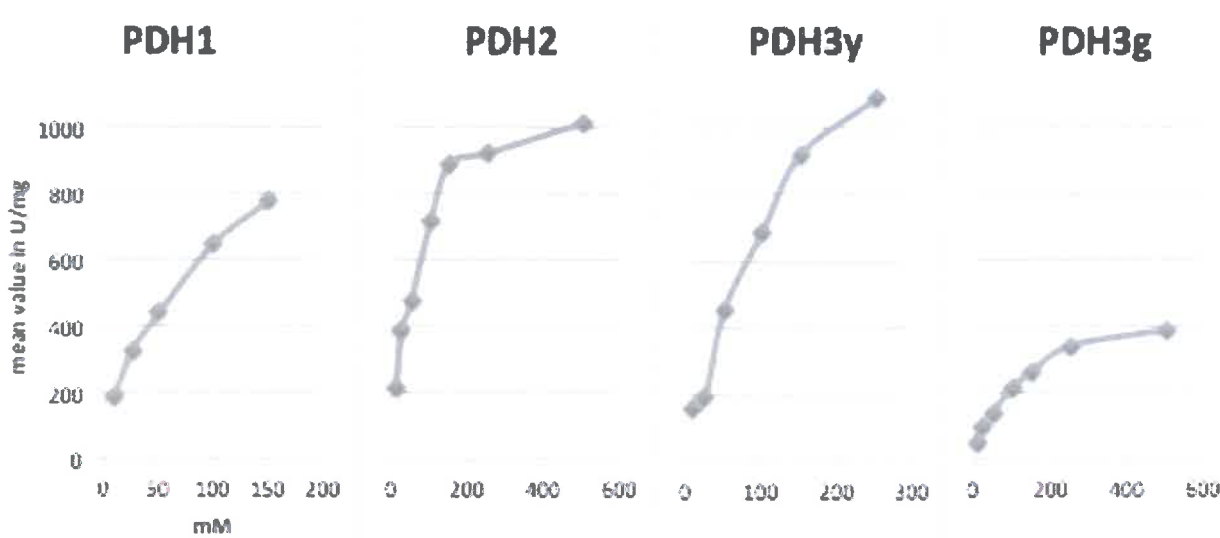


Figure 21: PDH isofomens with Maltotriose

3.3.2.7 Mannose

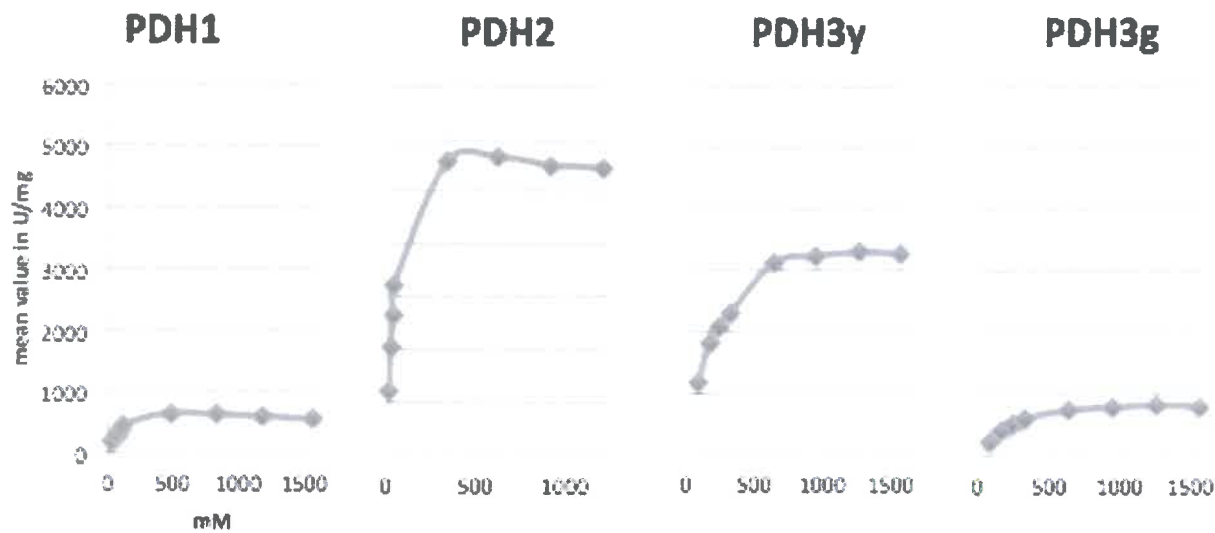


Figure 22: PDH isoforms with Mannose

3.3.2.8 Methyl- $\alpha$ -D-glucopyranosid

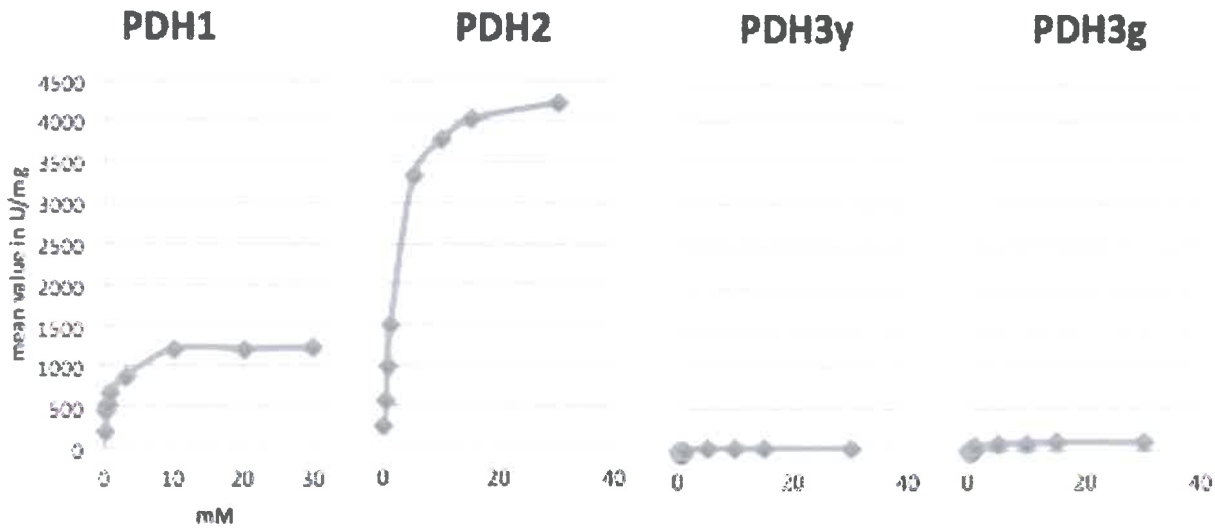
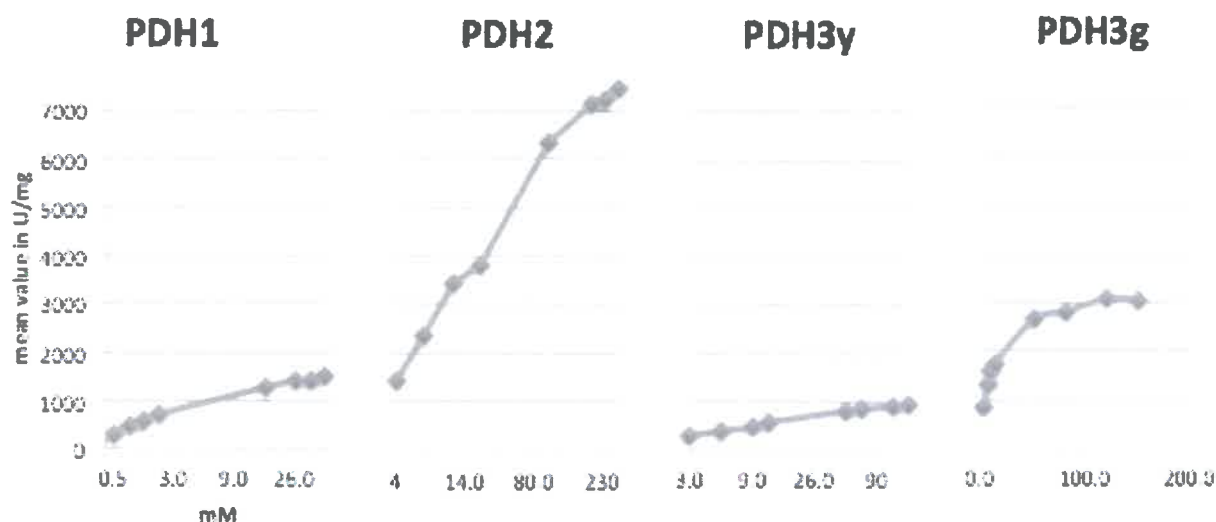


Figure 23: PDH isoforms with Methyl-  $\alpha$  -D-glucopyranoside

3.3.2.9 *D*-xyloseFigure 24: PDH isoforms with *D*-xylose

Catalytic constants were determined for selected sugar substrates. The most interesting apparent catalytic constants are those for glucose because the PDH isoforms could potentially be used in pacemakers (biofuel cell) or for measurements of the blood sugar level for diabetic patients (biofuel sensor). In both cases, blood glucose is the electron donor.

To compare the different isoforms the catalytic efficiencies ( $k_{cat}/K_m$ ) were used. The  $K_m$  value of PDH1 with *D*-glucose was very low and  $k_{cat}$  very high, resulting in a high catalytic efficiency of  $51.0 \text{ sec}^{-1} \cdot \text{mM}^{-1}$ . Therefore, the substrate is readily bound and rapidly converted to the final product before *D*-glucose can dissociate from the enzyme substrate–complex [7].

PDH1 had its best catalytic efficiency with methyl- $\alpha$ -*D*-glucopyranoside, PDH2 with *D*-glucose, PDH3y and PDH3g with *D*-xylose (Table 12–16).

PDH2 and PDH1 had the highest or second highest catalytic efficiency for *D*-glucose, respectively. Both, PDH3y and PDH3g, had a very small  $K_m$  value with *D*-glucose, however, due to their low  $k_{cat}$  their catalytic efficiency was very small ( $2.26 \text{ sec}^{-1} \cdot \text{mM}^{-1}$  for PDH3y and  $0.65 \text{ sec}^{-1} \cdot \text{mM}^{-1}$  for PDH3g).



The catalytic efficiency of PDH2 with di- and oligosaccharides was very low. This could be an evidence for a narrower active site or substrate channel compared to PDH1, which would hinder easy access of di- and oligosaccharides to the active site.

The catalytic efficiency of PDH2, PDH3g and PDH3y with lactose and D-maltose was very low. The catalytic efficiency with D-maltose was double the amount of maltotriose. Maltotriose is a trisaccharide and consists of three glucose molecules, whereas D-maltose consists of only two glucose molecules. Therefore, isoforms two and three have a slight preference for disaccharides ( $0.5 \times [k_{\text{cat}}/K_m]_{\text{D-maltose}} \sim 1 \times [k_{\text{cat}}/K_m]_{\text{maltotriose}}$ ), whereas PDH1 has a clear preference for disaccharides ( $0.1 \times [k_{\text{cat}}/K_m]_{\text{D-maltose}} \sim 1 \times [k_{\text{cat}}/K_m]_{\text{maltotriose}}$ ).

The catalytic efficiency with D-allose, which is a C3 epimer of D-glucose, was very small for all PDH isoforms, which can mainly be attributed to high  $K_m$  values. This indicates that the stereochemistry of the hydroxyl group attached to C3 of the hexose significantly affects the binding affinity to all three isoforms.

The catalytic efficiency of PDH1 and PDH2 with lactose is smaller than with D-maltose, whereas for both PDH3s it is higher. Lactose is a disaccharide composed of galactose and glucose, whereas D-maltose is composed of two glucose units. All three isoforms show high  $k_{\text{cat}}$  values for lactose, however, the  $K_m$  values were high for PDH3 and extremely high for PDH2 compared to PDH1, which results in poor catalytic efficiencies for isoforms two and three.

**Table 12: Apparent steady state constants of PDH1 with electron donors**

PDH1	$V_{\text{max}}$ ( $\mu\text{molmin}^{-1}\text{mg}^{-1}$ )	$K_m$ (mM)	$k_{\text{cat}}$ ( $\text{s}^{-1}$ )	$k_{\text{cat}}/K_m$ ( $\text{mM}^{-1}\text{s}^{-1}$ )
<b>D-allose</b>	523	16.9	17.5	1.03
<b>D-galactose</b>	1029	0.64	34.3	53.5
<b>D-glucose</b>	1261	0.82	42.1	51.0
<b>Lactose</b>	1010	76.7	33.7	0.44
<b>D-maltose</b>	1337	10.3	44.6	4.33
<b>Maltotriose</b>	1073	62.5	35.8	0.57
<b>D-mannose</b>	792	94.0	26.4	0.28

<b>Methyl-<math>\alpha</math>-D-glucopyranoside</b>	1240	0.66	41.4	62.3
<b>D-xylose</b>	1539	2.39	51.3	21.5

Table 13: Apparent steady state constants of PDH2 with electron donors

PDH2	$V_{\max}$ ( $\mu\text{molmin}^{-1}\text{mg}^{-1}$ )	$K_m$ (mM)	$k_{\text{cat}}$ ( $\text{s}^{-1}$ )	$k_{\text{cat}}/K_m$ ( $\text{mM}^{-1}\text{s}^{-1}$ )
<b>D-allose</b>	2151	113	40.0	0.35
<b>D-galactose</b>	7321	40.1	136	3.40
<b>D-glucose</b>	1912	0.53	35.5	67.1
<b>Lactose</b>	11069	2267	206	0.09
<b>D-maltose</b>	417	12.3	7.76	0.63
<b>Maltotriose</b>	1134	54.6	21.1	0.39
<b>D-mannose</b>	5861	35.0	109	3.12
<b>Methyl-<math>\alpha</math>-D-glucopyranoside</b>	4556	2.00	84.7	42.4
<b>D-xylose</b>	7803	16.96	145	8.55

Table 14: Apparent steady state constants of PDH3y with electron donors

PDH3y	$V_{\max}$ ( $\mu\text{molmin}^{-1}\text{mg}^{-1}$ )	$K_m$ (mM)	$k_{\text{cat}}$ ( $\text{s}^{-1}$ )	$k_{\text{cat}}/K_m$ ( $\text{mM}^{-1}\text{s}^{-1}$ )
<b>D-allose</b>	3868	181	34.7	0.19
<b>D-galactose</b>	1956	24.7	16.2	0.65
<b>D-glucose</b>	895	3.28	7.40	2.26
<b>Lactose</b>	8252	235	74.0	0.31
<b>D-maltose</b>	52.7	2.22	0.47	0.21
<b>Maltotriose</b>	1789	154	16.1	0.10
<b>D-mannose</b>	3801	185	34.1	0.18
<b>Methyl-<math>\alpha</math>-D-glucopyranoside</b>	110	0.95	0.99	1.04
<b>D-xylose</b>	3222	9.30	28.9	3.11

Table 15: Apparent steady state constants of PDH3g with electron donors

PDH3g	$V_{\max}$ ( $\mu\text{mol min}^{-1} \text{mg}^{-1}$ )	$K_m$ (mM)	$k_{\text{cat}}$ ( $\text{s}^{-1}$ )	$k_{\text{cat}}/K_m$ ( $\text{mM}^{-1} \text{s}^{-1}$ )
<b>D-allose</b>	1166	165	9.64	0.06
<b>D-galactose</b>	576	34.6	5.17	0.15
<b>D-glucose</b>	298	4.09	2.67	0.65
<b>Lactose</b>	2569	271	21.3	0.08
<b>D-maltose</b>	17.0	2.39	0.14	0.06
<b>Maltotriose</b>	481	115	3.98	0.03
<b>D-mannose</b>	972	206	8.04	0.04
<b>Methyl-<math>\alpha</math>-D-glucopyranoside</b>	34.3	1.17	0.28	0.24
<b>D-xylose</b>	959	8.53	7.93	0.93

## 4. Conclusion

PDH from various sources (e.g. *Agaricus xanthoderma*, *A. bisporus* and *A. meleagris*) were previously purified and characterized in detail by our group [5].

In the present study, we investigated three PDH isoforms from *A. meleagris*, namely PDH1, PDH2 and PDH3. Depending on the fermentation conditions, two differently colored batches of PDH3 were obtained: a yellow batch (depicted PDH3y) and a green batch (depicted PDH3g). For the majority of sugar substrates, PDH1 had the lowest  $K_m$  and the highest  $k_{cat}$  values, resulting in the highest catalytic efficiencies of all tested isoforms. In this respect, PDH2 was routinely ranked second and PDH3 last (PDH3y  $\sim 3 \times$  PDH3g). The values for PDH3y were most of the time about a fifth to one tenth of the values for PDH1. All isoforms reacted best with monosaccharides and not so well with di- and oligosaccharides. However, one should refrain from generalizations, because there were many peculiarities in the catalytic constants for the electron donors.

In contrast, the most striking differences in catalytic constants were observed for the tested electron acceptors (ABTS, BQ and  $Fc^+$ ), which points towards the physiological role of PDH2 and PDH3. Rather than being alternative enzymes for sugar oxidation and therefore lignin degradation, these two isoforms could be important for providing reduction equivalents for coupled enzyme systems involved in lignin degradation.

As a side note, it should be mentioned that we obtained first crystals of PDH2 and PDH3 in collaboration with Prof. Divne from KTH Stockholm. However, these crystals did not refract well and therefore, no three dimensional structure could be obtained of these isoforms.

## 5. References

- [1] C. K. Peterbauer and J. Volc, "Pyranose dehydrogenases: Biochemical features and perspectives of technological applications," *Applied Microbiology and Biotechnology*, vol. 85, no. 4, pp. 837–848, 2010.
- [2] R. Kittl, C. Sygmund, P. Halada, J. Volc, C. Divne, D. Haltrich, and C. K. Peterbauer, "Molecular cloning of three pyranose dehydrogenase-encoding genes from *Agaricus meleagris* and analysis of their expression by real-time RT-PCR," *Curr. Genet.*, vol. 53, no. 2, pp. 117–127, 2008.
- [3] B. Alberts, D. Bray, A. Johnson, and J. Lewis, *Lehrbuch der molekularen Zellbiologie*, 2nd ed. Wiley-VCH Weinheim, 2001.
- [4] C. Sygmund, R. Kittl, J. Volc, P. Halada, E. Kubátová, D. Haltrich, and C. K. Peterbauer, "Characterization of pyranose dehydrogenase from *Agaricus meleagris* and its application in the C-2 specific conversion of d-galactose," *J. Biotechnol.*, vol. 133, no. 3, pp. 334–342, 2008.
- [5] M. Kujawa, J. Volc, P. Halada, P. Sedmera, C. Divne, C. Sygmund, C. Leitner, C. Peterbauer, and D. Haltrich, "Properties of pyranose dehydrogenase purified from the litter-degrading fungus *Agaricus xanthoderma*," *FEBS J.*, vol. 274, no. 3, pp. 879–894, 2007.
- [6] I. Krondorfer, K. Lipp, D. Brugger, P. Staudigl, C. Sygmund, D. Haltrich, and C. K. Peterbauer, "Engineering of pyranose dehydrogenase for increased oxygen reactivity," *PLoS One*, vol. 9, no. 3, 2014.
- [7] L. Stryer, J. M. Berg, and J. L. Tymoczko, *Stryer Biochemistry*, 6th ed. Elsevier GmbH, München, 2007.
- [8] H. Bannwarth, B. P. Kremer, and A. Schulz, *Basiswissen Physik, Chemie und Biochemie*, 3rd ed. Springer-Spektrum, Berlin Heidelberg, 2013.
- [9] H. Bisswanger, *Enzymkinetik*, 3rd ed. Wiley-VCH, Weinheim, 2009.
- [10] Sigma Aldrich, "sigmaaldrich.com." [Online]. Available: [www.sigmaaldrich.com/catalog/product/roche/10102946001?lang=de&region=AT](http://www.sigmaaldrich.com/catalog/product/roche/10102946001?lang=de&region=AT).
- [11] H. J. Danneel, E. Rössner, A. Zeeck, and F. Giffhorn, "Purification and characterization of a pyranose oxidase from the basidiomycete *Peniophora gigantea* and chemical analyses of its reaction products," *Eur. J. Biochem.*, vol. 214, no. 3, pp. 795–802, 1993.

- [12] L. Pitulice, I. Pastor, E. Vilaseca, and et al., "Biotransformation Influence of Macromolecular Crowding on the Oxidation of ABTS by Hydrogen Peroxide Catalyzed by HRP," pp. 4–6, 2013.
- [13] S. Aldrich, "sigmaaldrich.com." [Online]. Available: <http://www.sigmaaldrich.com/catalog/product/aldrich/388297?lang=de&region=AT>.
- [14] Amersham and Amersham, "Protein and Peptide Purification Technique selection guide," *Amersham Biosci.*, pp. 1–7, 2003.
- [15] G. E. Healthcare, "Chromatography (Hydrophobic Interactions)."
- [16] GE Healthcare Life Sciences, "Handbook-No.: 28-9833-31 'Strategies for Protein Purification,'" 2014.
- [17] P. Christen and R. Jaussi, *Biochemie - Eine Einführung mit 40 Lerneinheiten*, 1st ed. Springer-Verlag Berlin Heidelberg, 2005.
- [18] M. Bradford, "Rapid and Sensitive Method for Quantification of Microgram Quantities of Protein utilizing principle of Protein-Dye-Binding.," *Anal. Biochem.*, vol. 72, no. 1–2, pp. 248–254, 1976.
- [19] S. Silbernagl, *Taschenatlas Physiologie*, 8th ed. Thieme.
- [20] M. M. H. Graf, U. Bren, D. Haltrich, and C. Oostenbrink, "Molecular dynamics simulations give insight into d-glucose dioxidation at C2 and C3 by *Agaricus meleagris* pyranose dehydrogenase," *J. Comput. Aided. Mol. Des.*, vol. 27, no. 4, pp. 295–304, 2013.

## 6. Curriculum vitae

### PERSONAL DATA

Name: Sandra Weber  
Date of birth: 03. October 1987  
Address: Praterstraße 76/12 A-1020 Vienna  
E-mail: [sandra@mxr.at](mailto:sandra@mxr.at)

### EDUCATION

**University of Natural Resources and Life Sciences,  
Vienna**  
Gregor Mendel Straße 33 A-1180 Vienna ☐  
Since 05/2011 **Master:** Lebensmittelwissenschaft u. -technologie - (H 066  
417) ☐  
10/2006 – 04/2011 **Bachelor:** Lebensmittel und Biotechnologie - (H 033 217)  
  
09/1998 – 06/2006 **Gymnasium und wirtschaftskundliches Realgymnasium  
Der Dominikanerinnen**  
Schloßberggasse 17 A-1130 Wien ☐

### WORK EXPERIENCE

03/13 – 04/13 **Karolinska Institutet**, Stockholm  
Department: Medical Biochemistry and Biophysics  
Workgroup: Christina Divne  
  
07/08 – 09/08 **Medizinische Universität Wien, AKH**, Vienna  
Department: Clin. Med. Chem. Laboratory Diagnostics  
Workgroup: Markus Kubicek  
  
Since 2005 **MXR Productions GmbH**, Vienna  
Filmproduction  
Department: Production Management

## **Eidesstattliche Erklärung**

Ich erkläre hiermit an Eides Statt, dass ich die vorliegende Arbeit selbstständig und ohne Benutzung anderer als der angegebenen Hilfsmittel angefertigt habe. Die aus fremden Quellen direkt oder indirekt übernommenen Gedanken sind als solche kenntlich gemacht.

Die Arbeit wurde bisher in gleicher oder ähnlicher Form keiner anderen Prüfungsbehörde vorgelegt und auch noch nicht veröffentlicht.

Wien am 18.09. 2015